

Supporting Information

Engineering of alkyl chain branching point on a lactone polymer donor yields 17.81% efficiency

Zongliang Ou,^{‡ab} Jianqiang Qin,^{‡bd} Ke Jin,^b Jianqi Zhang,^b Lixiu Zhang,^b Chenyi Yi,^e Zhiwen Jin,^f Qiuling Song,^{*a} Kuan Sun,^{*d} Junliang Yang,^{*c} Zuo Xiao^{*b} and Liming Ding^{*b}

^a *Institute of Next Generation Matter Transformation, College of Materials Science & Engineering, Huaqiao University, Xiamen 361021, China. E-mail: qsong@hqu.edu.cn*

^b *Center for Excellence in Nanoscience, Key Laboratory of Nanosystem and Hierarchical Fabrication (CAS), National Center for Nanoscience and Technology, Beijing 100190, China. E-mail: xiaoz@nanoctr.cn; ding@nanoctr.cn*

^c *State Key Laboratory of Powder Metallurgy, School of Physics and Electronics, Central South University, Changsha 410083, China. E-mail: junliang.yang@csu.edu.cn*

^d *Key Laboratory of Low-grade Energy Utilization Technologies and Systems (MOE), School of Energy and Power Engineering, Chongqing University, Chongqing 400044, China. E-mail: kuan.sun@cqu.edu.cn*

^e *Department of Electrical Engineering, Tsinghua University, Beijing 100084, China.*

^f *School of Physical Science and Technology, Lanzhou University, Lanzhou 730000, China.*

[‡] Z. Ou and J. Qin contributed equally to this work.

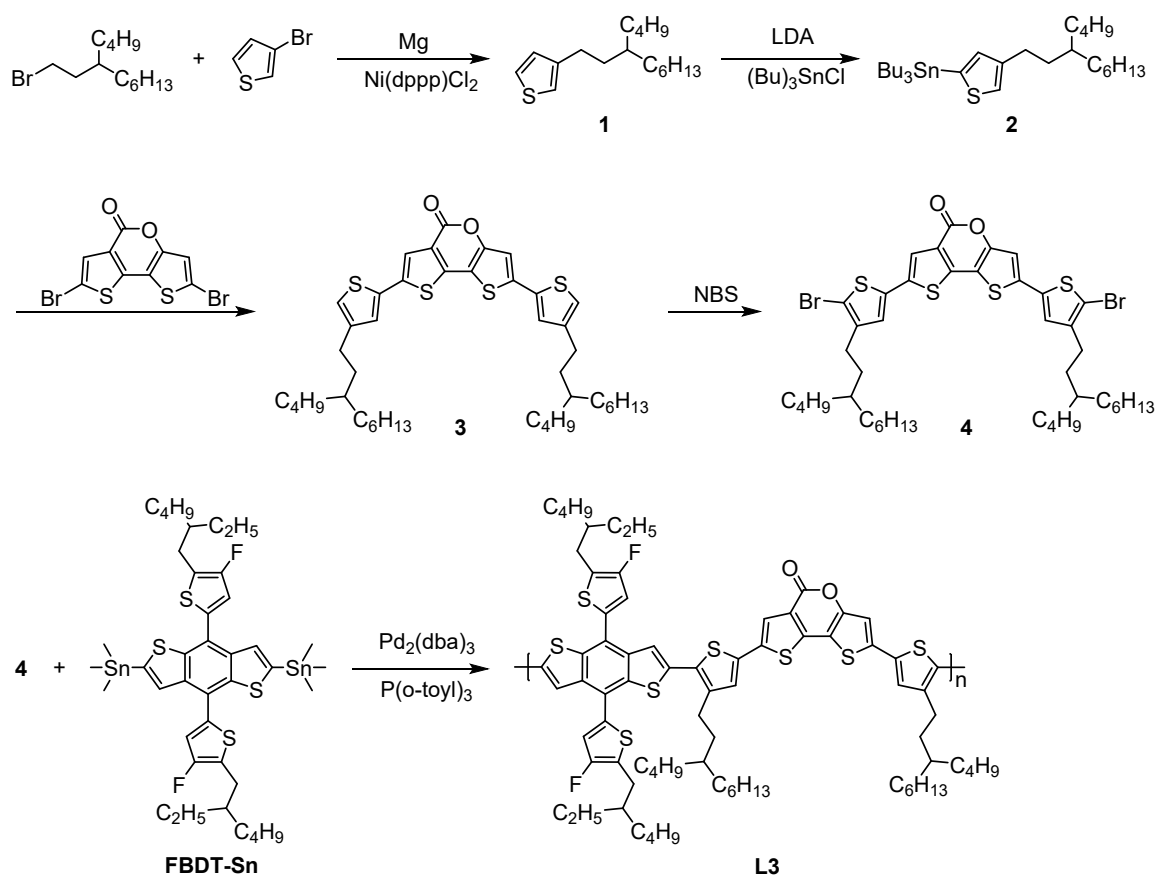
* Corresponding authors.

1. General characterization

^1H and ^{13}C NMR spectra were measured on a Bruker Avance-400 spectrometer. Absorption spectra were recorded on a Shimadzu UV-1800 spectrophotometer. Cyclic voltammetry was done by using a Shanghai Chenhua CHI620D voltammetric analyzer under argon in an anhydrous acetonitrile solution of tetra-*n*-butylammonium hexafluorophosphate (0.1 M). A glassy-carbon electrode was used as the working electrode, a platinum-wire was used as the counter electrode, and a Ag/Ag^+ electrode was used as the reference electrode. Polymers were coated onto glassy-carbon electrode and all potentials were corrected against Fc/Fc^+ . Grazing-incidence wide-angle X-ray scattering (GIWAXS) was done on a Xeuss SAXS/WAXS instrument. L2:N3 (1:1.2), L3:N3 (1:1.2), L3:N3:PC₆₁BM (1:1.2:0.2) blend films were deposited onto PEDOT:PSS/Si substrates via spin-coating. AFM was performed on a Multimode microscope (Veeco) using tapping mode.

2. Synthesis

All reagents were purchased from J&K Co., Aladdin Co., Innochem Co., Derthon Co., SunaTech Co. and other commercial suppliers. N3 was purchased from eFlexPV Co. 2,7-Dibromo-5H-dithieno[3,2-*b*:2',3'-*d*]pyran-5-one and L2 were prepared according to literature.^[1] All reactions dealing with air- or moisture-sensitive compounds were carried out by using standard Schlenk techniques.



Scheme S1 The synthetic route for L3.

Compound 1. To magnesium turning (107 mg, 4.42 mmol) in dry THF (3 mL) was added 1-bromo-3-butyl nonane (970 mg, 3.68 mmol) dropwise under nitrogen. The reaction mixture was refluxed for 1 h. The Grignard reagent was cooled and then added dropwise to 3-bromothiophene (500 mg, 3.07 mmol) and Ni(dppp)Cl₂ (43 mg, 0.08 mmol). The solution was heated to reflux and stirred overnight and quenched by H₂O. The solution was extracted by petroleum ether, washed by saturated aqueous NaCl, and dried over MgSO₄. The organic phase after evaporation was purified by column chromatography (silica gel, hexane) to give **compound 1** as a colorless oil (597 mg, 73%). ¹H NMR (CDCl₃, 400 MHz, δ/ppm): 7.20-7.22 (m, 1H), 6.93 (dd, *J* = 4.9, 1.1 Hz, 1H), 6.90 (dd, *J* = 2.8, 1.0 Hz, 1H), 2.60 (dd, *J* = 9.4, 6.9 Hz, 2H), 1.53-1.61 (m, 2H), 1.26 (m, 17H), 0.88 (m, 6H). ¹³C NMR (CDCl₃, 100 MHz, δ/ppm): 143.52, 128.25, 125.02, 119.56, 37.11, 34.51, 33.54, 33.22, 31.95, 29.80, 28.88, 27.53, 26.61, 23.15, 22.72, 14.16, 14.12.

Compound 2. To a solution of compound 1 (300 mg, 1.13 mmol) in THF (6 mL) was added lithium diisopropylamide (2 M, 1.47 mmol) at -78 °C under nitrogen. After stirring at the same temperature for 2 h, tributylstannyl chloride (394 mg, 1.24 mmol) was added to the mixture, and the mixture was warmed to room temperature. After stirring overnight, the mixture was quenched with water (15 mL) and extracted with petroleum ether. The organic layer was dried with MgSO₄, and the crude **compound 2** was obtained by removing the solvent and used directly for the next step.

Compound 3. To a solution of 2,7-dibromo-5H-dithieno[3,2-b:2',3'-d]pyran-5-one (150 mg, 0.41 mmol) and compound 2 (524 mg, 0.94 mmol) in toluene (4 mL) and DMF (1 mL) was added Pd(PPh₃)₄ (47 mg, 0.041 mmol) under nitrogen. The mixture was heated to reflux for 12 h. After cooling to room temperature, the mixture was poured into saturated aqueous NaCl and extracted with petroleum ether for three times. The combined organic layer was dried over anhydrous Na₂SO₄, filtered, and evaporated. The residue was purified via column chromatography (silica gel) by using CH₂Cl₂:petroleum ether (1:1) as eluent to give **compound 3** as a yellow solid (250 mg, 83%). ¹H NMR (CDCl₃, 400 MHz, δ/ppm): 7.57 (s, 1H), 7.11 (d, *J* = 1.2 Hz, 1H), 7.06 (d, *J* = 1.2 Hz, 1H), 7.05 (s, 1H), 6.93 (d, *J* = 0.8 Hz, 1H), 6.89 (d, *J* = 0.8 Hz, 1H), 2.54-2.61 (m, 4H), 1.56-1.62 (m, 4H), 1.25-1.35 (m, 34H), 0.87-0.93 (m, 12H). ¹³C NMR (CDCl₃, 100 MHz, δ/ppm): 157.47, 152.51, 144.99, 144.78, 143.28, 137.90, 135.96, 135.43, 135.01, 126.48, 126.44, 122.36, 121.35, 121.19, 120.66, 113.03, 111.43, 37.08, 34.34, 33.48, 33.16, 31.93, 29.78, 28.86, 27.69, 26.59, 23.13, 22.71, 14.17, 14.13.

Compound 4. To a solution of compound 3 (200 mg, 0.27 mmol) in CHCl₃ (5 mL) and DMF (1 mL) was added NBS (98 mg, 0.55 mmol) at room temperature. The mixture was stirred for 1 h. After removal of the solvent, the crude product was purified via column chromatography (silica gel) by using CHCl₃:petroleum ether (1:2) as eluent to give **compound 4** as a claybank solid (222 mg, 92%). ¹H NMR (CDCl₃, 400 MHz, δ/ppm): 7.48 (s, 1H), 6.97 (s, 1H), 6.95 (s, 1H), 6.90 (s, 1H), 2.49-2.55 (m, 4H), 1.51-1.57 (m, 4H), 1.29 (m, 34H), 0.91 (m, 12H). ¹³C NMR (CDCl₃, 100 MHz, δ/ppm): 157.13, 152.54, 143.93, 143.69, 143.11, 136.88, 135.13,

135.04, 134.74, 125.85, 125.83, 122.50, 121.65, 113.18, 111.49, 110.34, 109.72, 37.15, 37.13, 33.48, 33.42, 33.10, 31.95, 29.77, 28.86, 26.90, 26.60, 23.13, 22.72, 14.19, 14.14.

L3. To a mixture of compound 4 (72.3 mg, 0.08 mmol), FBDT-Sn (76.0 mg, 0.08 mmol), Pd₂(dba)₃ (2.2 mg, 0.0024 mmol) and P(o-Tol)₃ (7.4 mg, 0.024 mmol) in a Schlenk flask was added toluene (1.5 mL) under argon. The mixture was heated to reflux for 17 h. Then the solution was cooled to room temperature and added into 150 mL methanol dropwise. The precipitate was collected and further purified via Soxhlet extraction by using CH₂Cl₂:CHCl₃ (1:1), CHCl₃ and chlorobenzene in sequence. The chlorobenzene fraction was concentrated and added into methanol dropwise. The precipitate was collected and dried under vacuum overnight to give **L3** as a brown solid (65 mg, 60%). The Mn for L3 is 42.3 kDa, with a PDI of 1.64. ¹H NMR (CDCl₃, 400 MHz, δ/ppm): 6.66 (br, aromatic protons), 2.81 (br, aliphatic protons), 0.67-1.54 (br, aliphatic protons).

3. NMR

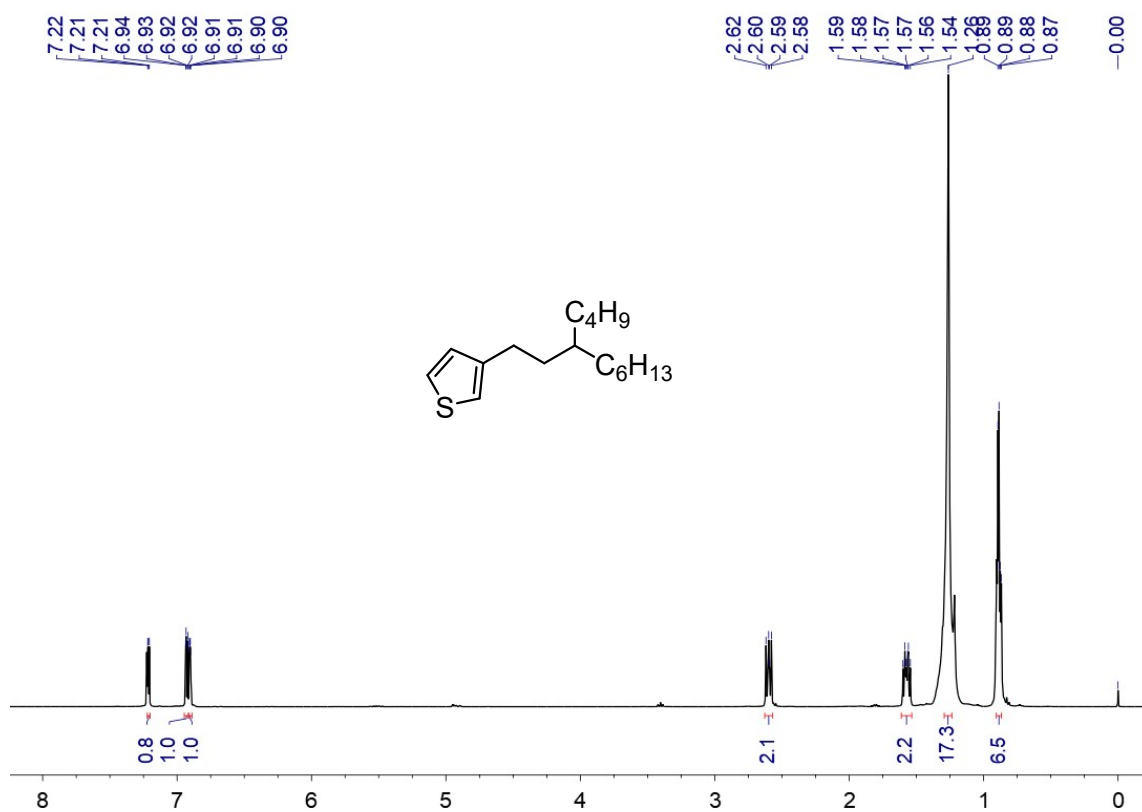


Fig. S1 ¹H NMR spectrum of compound 1.

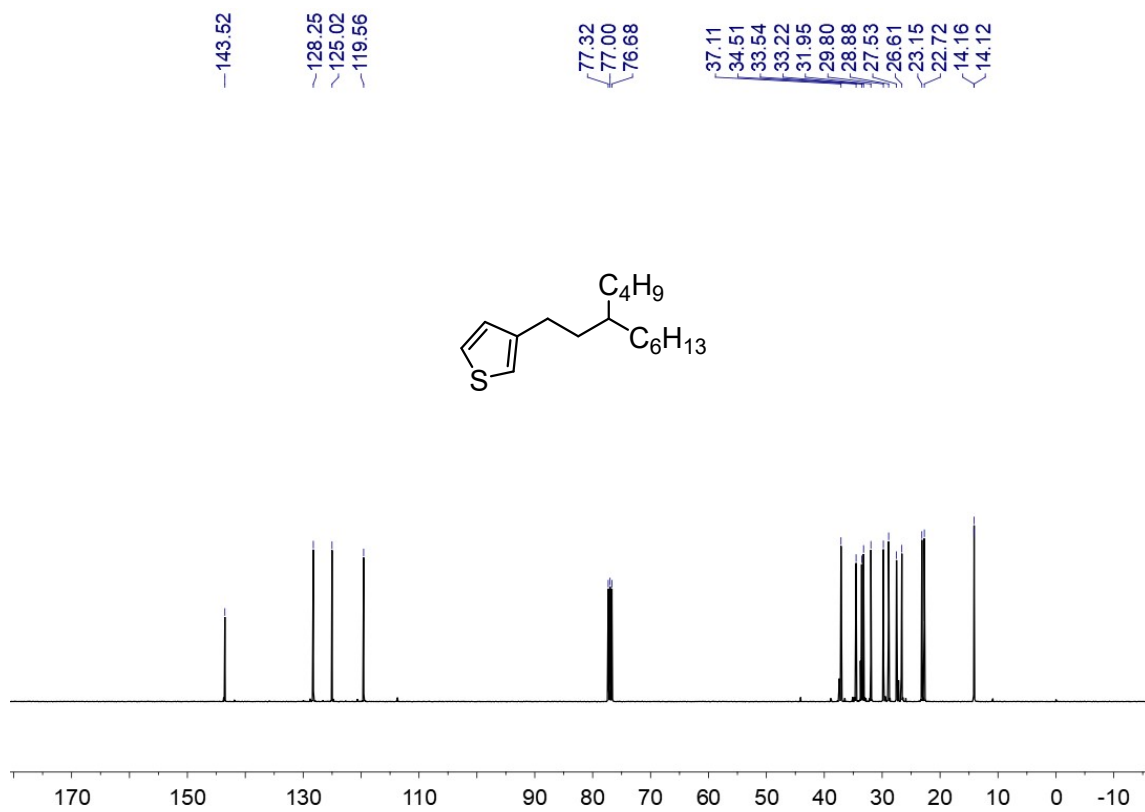


Fig. S2 ¹³C NMR spectrum of compound 1.

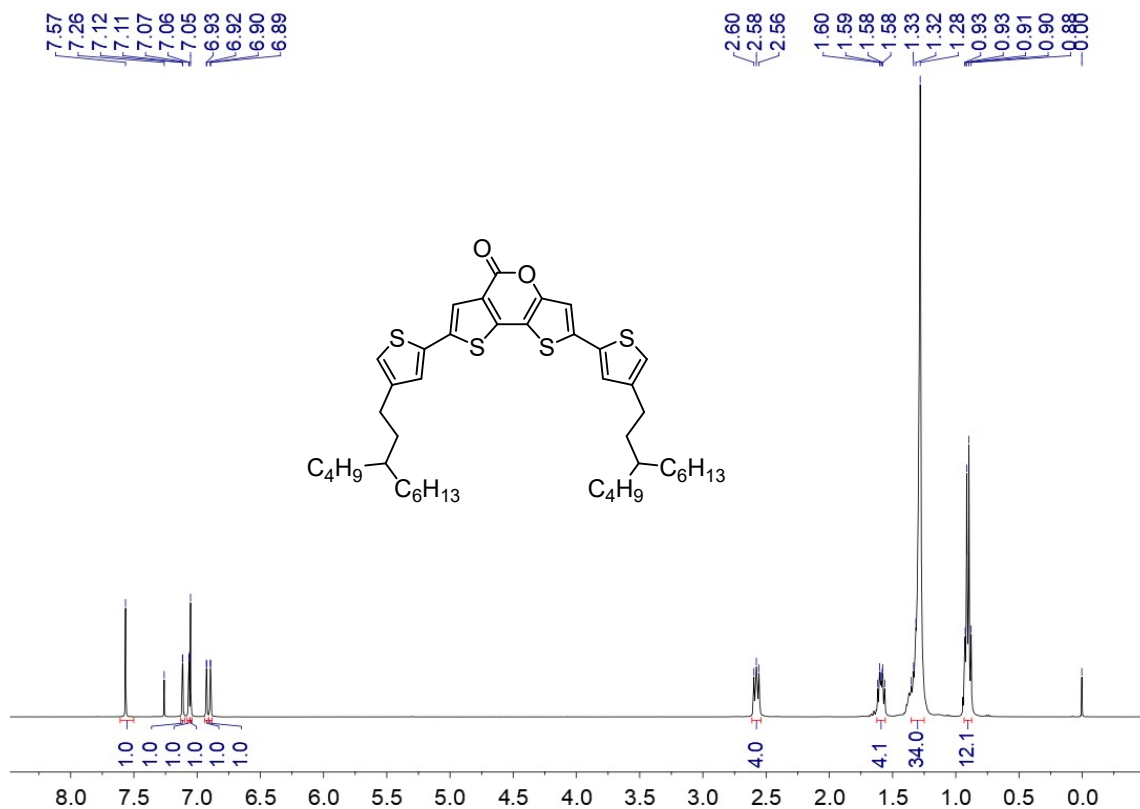


Fig. S3 ¹H NMR spectrum of **compound 3**.

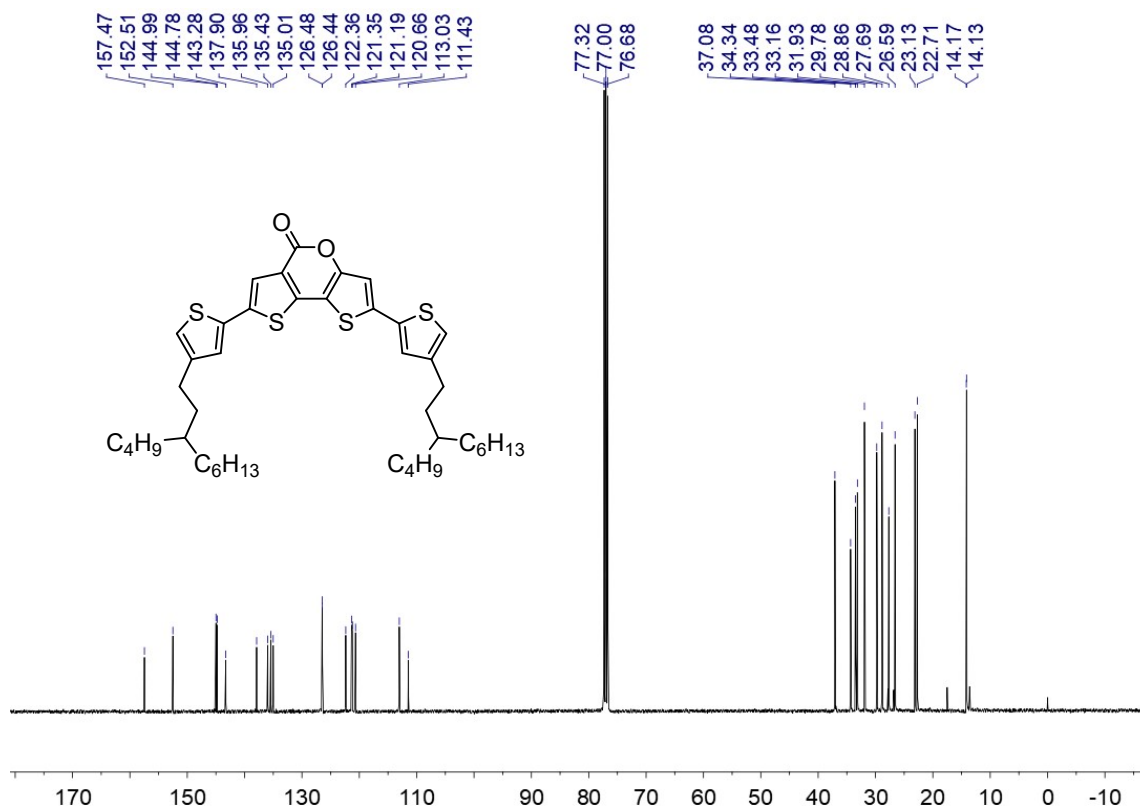


Fig. S4 ¹³C NMR spectrum of **compound 3**.

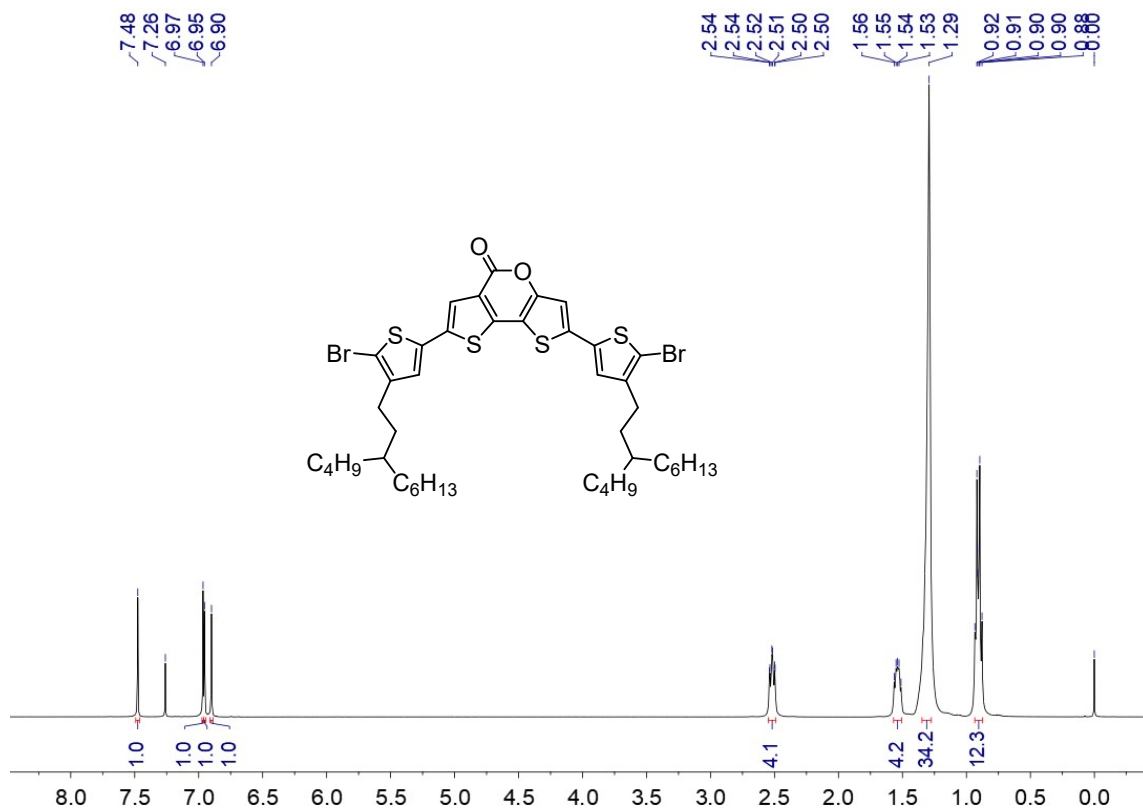


Fig. S5 ^1H NMR spectrum of compound 4.

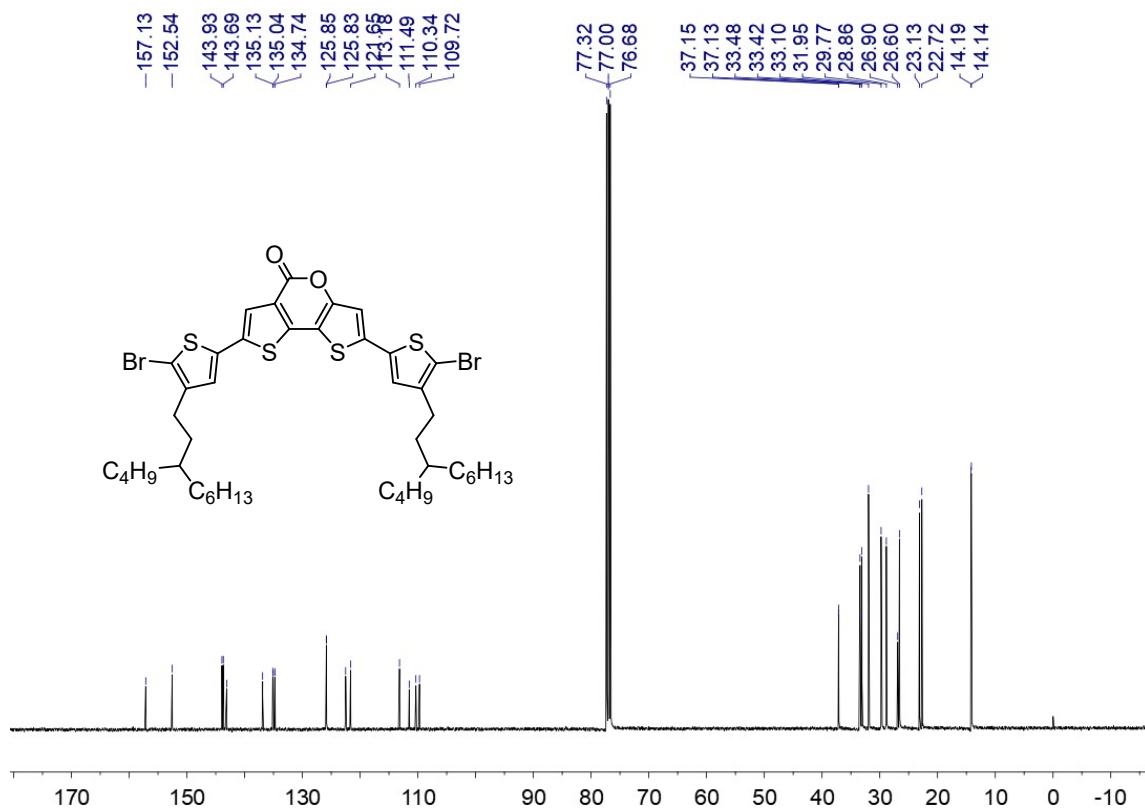


Fig. S6 ^{13}C NMR spectrum of compound 4.

4. CV

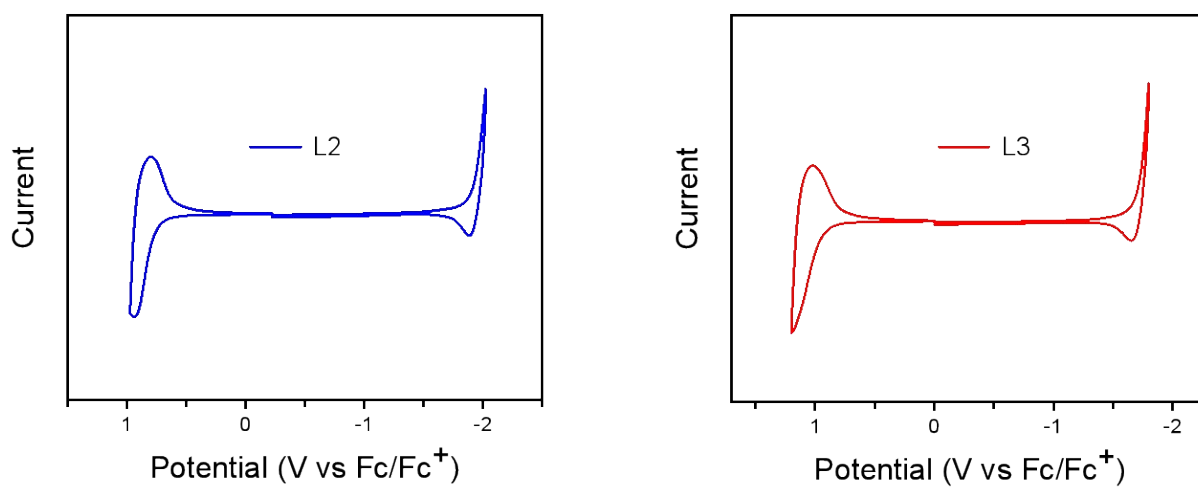


Fig. S9 Cyclic voltammograms for L2 and L3.

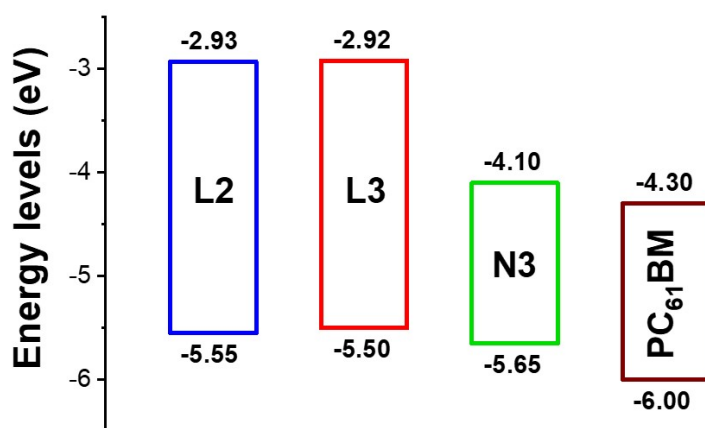
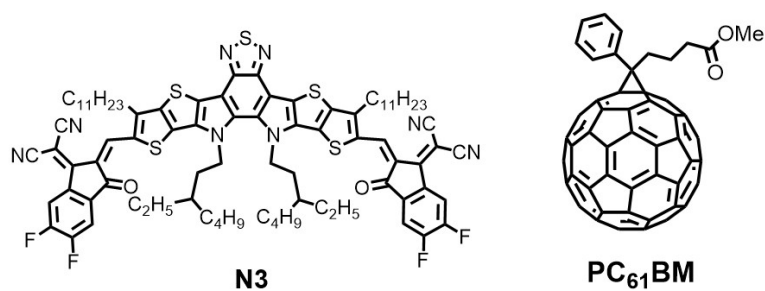


Fig. S10 Chemical structures of N3 and PC₆₁BM, and an energy level diagram.

5. A DFT model for the distant-from-backbone manipulation

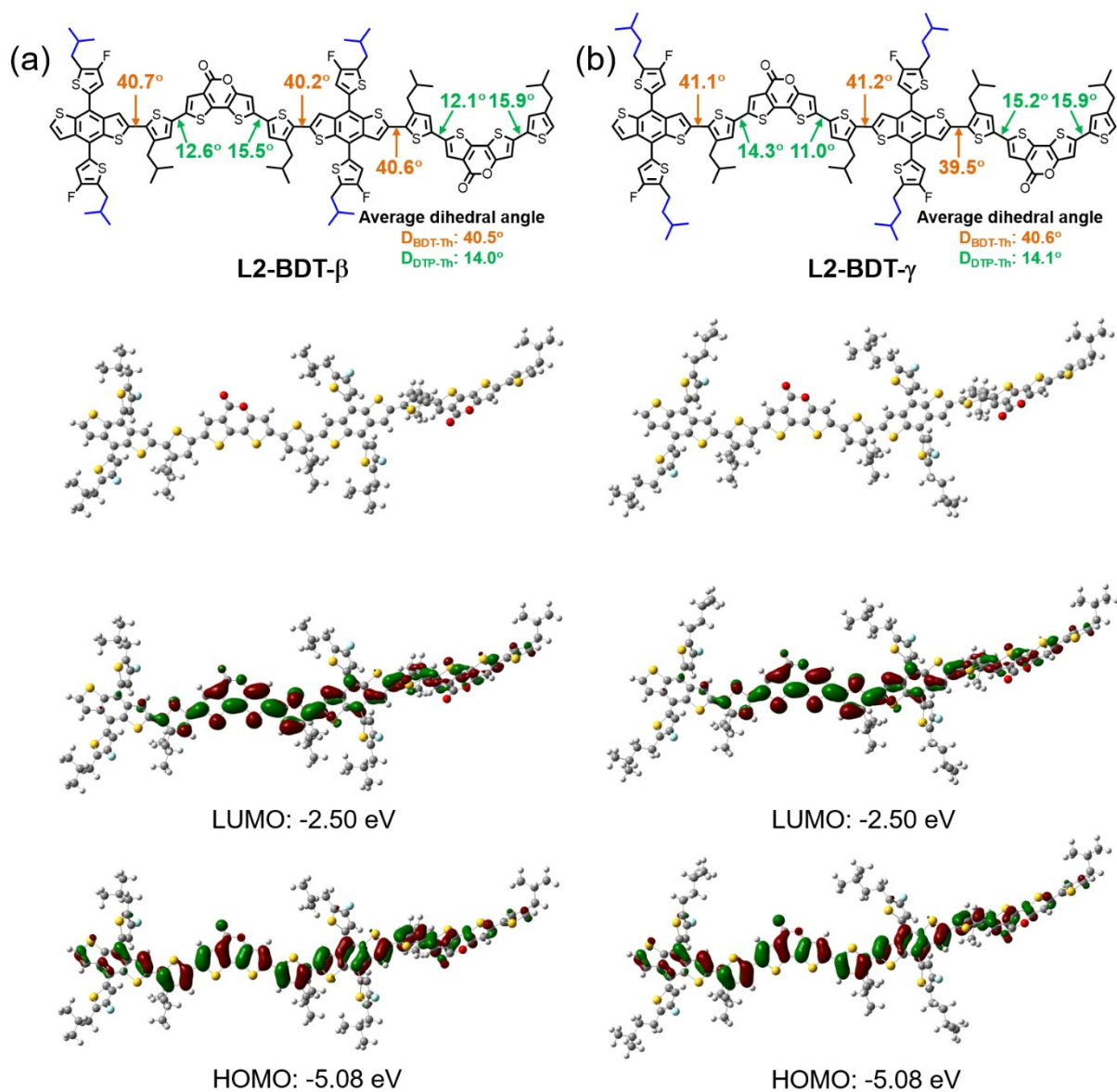


Fig. S11 Molecular model, optimized geometry, LUMO and HOMO for (a) L2-BDT- β and (b) L2-BDT- γ .

6. GIWAXS data

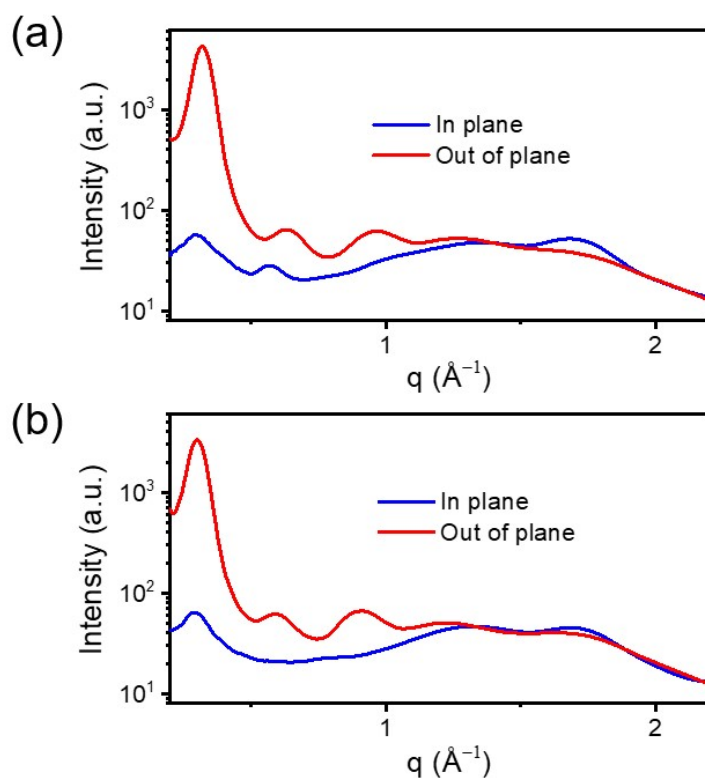


Fig. S12 OOP and IP profiles of the GIWAXS patterns for (a) pure L2 and (b) pure L3 films.

Table S1 Summary of d -spacings and CCLs for pure L2 and L3 films.

Films	d -spacing ₁₀₀ (OOP) [Å]	CCL ₁₀₀ (OOP) [Å]	d -spacing ₀₁₀ (IP) [Å]	CCL ₀₁₀ (IP) [Å]
L2	19.55	73.53	3.74	26.00
L3	20.77	68.49	3.74	25.55

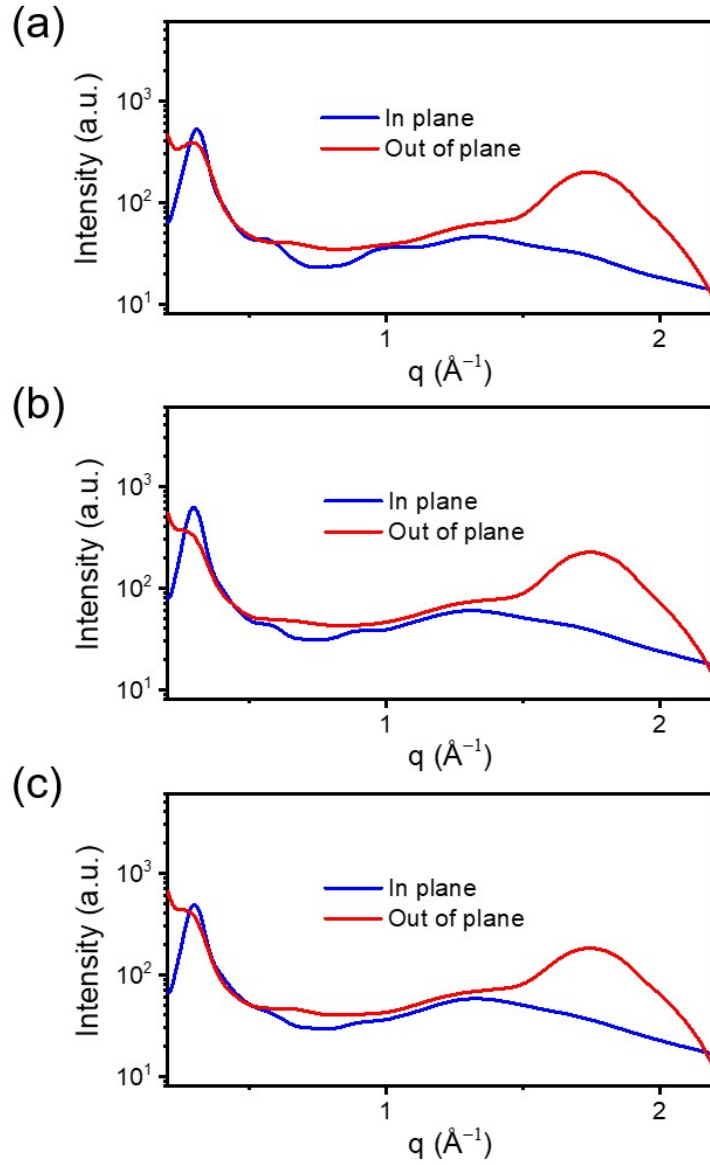


Fig. S13 OOP and IP profiles of the GIWAXS patterns for (a) L2:N3, (b) L3:N3 and (c) L3:N3:PC₆₁BM blend films.

Table S2 Summary of *d*-spacings and CCLs for L2:N3 (1:1.2), L3:N3 (1:1.2) and L3:N3:PC₆₁BM (1:1.2:0.2) blend films.

Films	<i>d</i> -spacing ₀₁₀ (OOP) [Å]	CCL ₀₁₀ (OOP) [Å]	<i>d</i> -spacing ₁₀₀ (IP) [Å]	CCL ₁₀₀ (IP) [Å]
L2:N3	3.61	20.78	20.39	67.07
L3:N3	3.60	21.09	21.09	72.26
L3:N3:PC ₆₁ BM	3.61	23.00	20.91	69.74

7. Device fabrication and measurements

Conventional solar cells

A 30 nm thick PEDOT:PSS layer was made by spin-coating an aqueous dispersion onto ITO glass (4000 rpm for 30 s). PEDOT:PSS substrates were dried at 150 °C for 10 min. A active blend in chloroform (CF) was spin-coated onto PEDOT:PSS layer. PDIN (2 mg/mL) in MeOH:AcOH (1000:3) was spin-coated onto active layer (5000 rpm for 30 s). Ag (~80 nm) was evaporated onto PDIN through a shadow mask (pressure ca. 10^{-4} Pa). The effective area for the devices is 4 mm². The thicknesses of the active layers were measured by using a KLA Tencor D-120 profilometer. $J-V$ curves were measured by using a computerized Keithley 2400 SourceMeter and a Xenon-lamp-based solar simulator (Enli Tech, AM 1.5G, 100 mW/cm²). The illumination intensity of solar simulator was determined by using a monocrystalline silicon solar cell (Enli SRC2020, 2cm×2cm) calibrated by NIM. The external quantum efficiency (EQE) spectra were measured by using a QE-R3011 measurement system (Enli Tech). The best cells were further tested at NIM for certification. A metal mask with an aperture (2.580 mm²) was used to define the effective area.

Hole-only devices

The structure for hole-only devices is ITO/PEDOT:PSS/active layer/MoO₃/Al. A 30 nm thick PEDOT:PSS layer was made by spin-coating an aqueous dispersion onto ITO glass (4000 rpm for 30 s). PEDOT:PSS substrates were dried at 150 °C for 10 min. Pure L2 (or L3) or a L2:N3 (or L3:N3; or L3:N3:PC₆₁BM) blend in CF was spin-coated onto PEDOT:PSS layer. Finally, MoO₃ (~6 nm) and Al (~100 nm) was successively evaporated onto the active layer through a shadow mask (pressure ca. 10^{-4} Pa). $J-V$ curves were measured by using a computerized Keithley 2400 SourceMeter in the dark.

Electron-only devices

The structure for electron-only devices is Al/active layer/Ca/Al. Al (~80 nm) was evaporated onto a glass substrate. A L2:N3 (or L3:N3; or L3:N3:PC₆₁BM) blend in CF was spin-coated onto Al. Ca (~5 nm) and Al (~100 nm) were successively evaporated onto the active layer through a shadow mask (pressure ca. 10^{-4} Pa). $J-V$ curves were measured by using a computerized Keithley 2400 SourceMeter in the dark.

8. Optimization of device performance

Table S3 Optimization of D/A ratio for L2:N3 conventional solar cells.^a

D/A [w/w]	V_{oc} [V]	J_{sc} [mA/cm ²]	FF [%]	PCE [%]
1:0.8	0.880	24.09	74.1	15.72 (15.63) ^b
1:1.2	0.880	24.42	74.6	16.03 (15.84)
1:1.6	0.882	22.93	75.2	15.21 (14.98)
1:2	0.882	21.54	74.4	14.14 (13.88)

^aBlend solution: 13.5 mg/mL in CF; spin-coating: 4000 rpm for 30 s.

^bData in parentheses are averages for 10 cells.

Table S4 Optimization of active layer thickness for L2:N3 conventional solar cells.^a

Thickness [65]	V_{oc} [V]	J_{sc} [mA/cm ²]	FF [%]	PCE [%]
122	0.881	24.22	74.6	15.93 (15.79) ^b
108	0.880	24.42	74.6	16.03 (15.84)
92	0.881	23.72	75.5	15.78 (15.44)
85	0.879	22.07	75.8	14.69 (14.51)

^aD/A ratio: 1:1.2 (w/w); blend solution: 13.5 mg/mL in CF.

^bData in parentheses are averages for 10 cells.

Table S5 Optimization of DPE content for L2:N3 conventional solar cells.^a

DPE [vol%]	V_{oc} [V]	J_{sc} [mA/cm ²]	FF [%]	PCE [%]
0	0.880	24.42	74.6	16.03 (15.84) ^b
0.2	0.872	24.56	76.6	16.41 (16.22)
0.5	0.871	24.78	76.7	16.57 (16.32)
0.8	0.870	24.99	76.8	16.69 (16.37)
1.2	0.866	24.62	75.3	16.05 (15.69)

^aD/A ratio: 1:1.2 (w/w); blend solution: 13.5 mg/mL in CF; spin-coating: 4000 rpm for 30 s.

^bData in parentheses are averages for 10 cells.

Table S6 Optimization of D/A ratio for L3:N3 conventional solar cells.^a

D/A [w/w]	V_{oc} [V]	J_{sc} [mA/cm ²]	FF [%]	PCE [%]
1:0.8	0.866	24.02	72.2	15.01 (14.94) ^b
1:1.2	0.865	25.43	75.8	16.67 (16.49)
1:1.6	0.865	24.61	75.5	16.08 (15.90)
1:2	0.867	23.44	75.2	15.29 (15.11)

^aBlend solution: 13.5 mg/mL in CF; spin-coating: 4000 rpm for 30 s.

^bData in parentheses are averages for 10 cells.

Table S7 Optimization of active layer thickness for L3:N3 conventional solar cells.^a

Thickness [65]	V_{oc} [V]	J_{sc} [mA/cm ²]	FF [%]	PCE [%]
125	0.862	24.64	74.9	15.91 (15.53) ^b
111	0.865	25.43	75.8	16.67 (16.49)
98	0.866	25.10	75.8	16.48 (16.20)
88	0.867	24.55	76.2	16.21 (15.84)

^aD/A ratio: 1:1.2 (w/w); blend solution: 13.5 mg/mL in CF.

^bData in parentheses are averages for 10 cells.

Table S8 Optimization of DPE content for L3:N3 conventional solar cells.^a

DPE [vol%]	V_{oc} [V]	J_{sc} [mA/cm ²]	FF [%]	PCE [%]
0	0.865	25.43	75.8	16.67 (16.49) ^b
0.2	0.861	25.80	76.4	16.97 (16.87)
0.5	0.860	26.39	75.9	17.23 (16.93)
0.8	0.857	26.02	76.1	16.98 (16.73)
1.2	0.852	26.20	75.3	16.80 (16.59)

^aD/A ratio: 1:1.2 (w/w); blend solution: 13.5 mg/mL in CF; spin-coating: 4000 rpm for 30 s.

^bData in parentheses are averages for 10 cells.

Table S9 Optimization of D/A₁/A₂ ratio for L3:N3:PC₆₁BM conventional solar cells.^a

D/A ₁ /A ₂ [w/w/w]	V _{oc} [V]	J _{sc} [mA/cm ²]	FF [%]	PCE [%]
1:1.2:0	0.860	26.39	75.9	17.23 (16.93) ^b
1:1.2:0.1	0.856	26.82	76.6	17.59 (17.20)
1:1.2:0.2	0.864	26.97	76.4	17.81 (17.45)
1:1.2:0.4	0.856	26.86	75.6	17.38 (16.97)
1:1.2:0.6	0.862	26.12	74.1	16.67 (16.42)

^aBlend solution: 13.5 mg/mL in CF with 0.5 vol% DPE; spin-coating: 4000 rpm for 30 s.

^bData in parentheses are averages for 10 cells.

9. SCLC

Charge carrier mobility was measured by SCLC method. The mobility was determined by fitting the dark current to the model of a single carrier SCLC, which is described by:

$$J = \frac{9}{8} \varepsilon_0 \varepsilon_r \mu \frac{V^2}{d^3}$$

where J is the current density, μ is the zero-field mobility of holes (μ_h) or electrons (μ_e), ε_0 is the permittivity of the vacuum, ε_r is the relative permittivity of the material, d is the thickness of the blend film, and V is the effective voltage ($V = V_{\text{appl}} - V_{\text{bi}}$, where V_{appl} is the applied voltage, and V_{bi} is the built-in potential determined by electrode work function difference). Here, $V_{\text{bi}} = 0.1$ V for hole-only devices, $V_{\text{bi}} = 0$ V for electron-only devices.^[2] The mobility was calculated from the slope of $J^{1/2}$ - V plot.

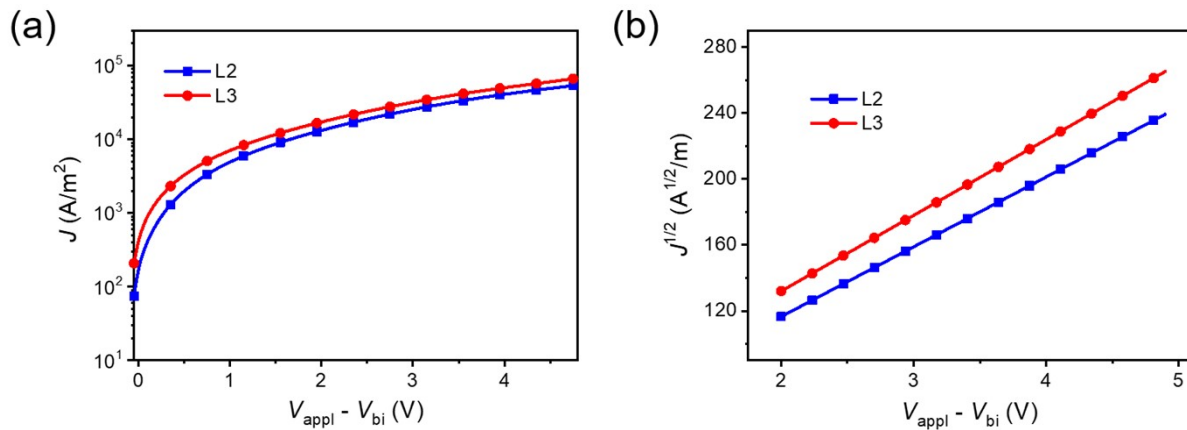


Fig. S14 J - V curve (a) and corresponding $J^{1/2}$ - V plot (b) for the hole-only devices (in dark). The thickness for L2 and L3 are 103 and 110 nm, respectively.

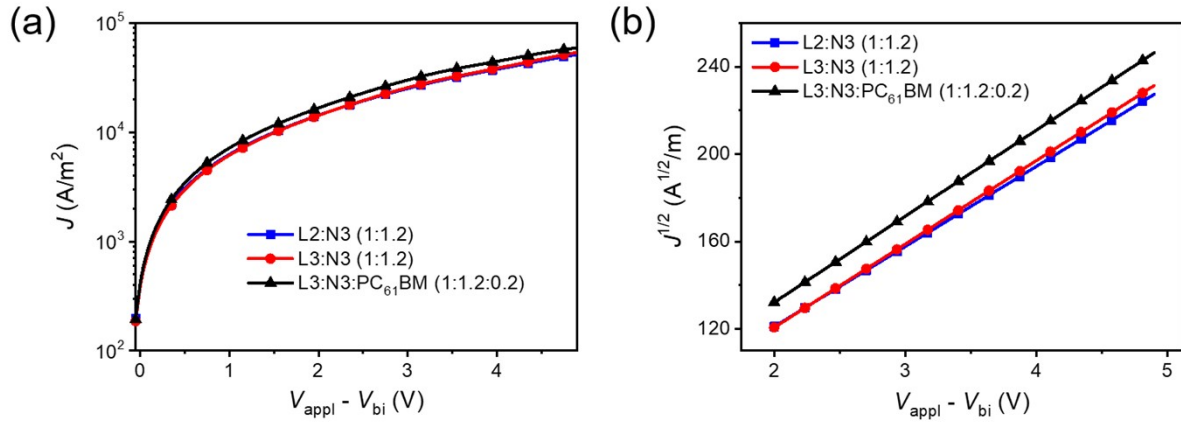


Fig. S15 J - V curve (a) and corresponding $J^{1/2}$ - V plot (b) for the hole-only devices (in dark). The thickness for L2:N3, L3:N3 and L3:N3:PC₆₁BM are 106, 109 and 109 nm, respectively.

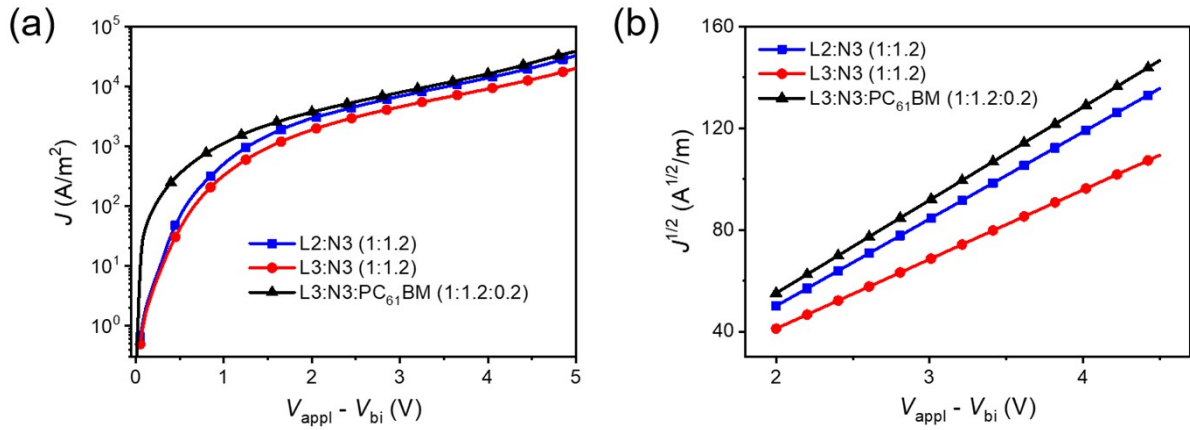


Fig. S16 J - V curve (a) and corresponding $J^{1/2}$ - V plot (b) for the electron-only devices (in dark). The thickness for L2:N3, L3:N3 and L3:N3:PC₆₁BM are 108, 110 and 112 nm, respectively.

Table S10 Hole and electron mobility.

Films	μ_h [cm ² /Vs]	μ_e [cm ² /Vs]	μ_h/μ_e
L2	6.54×10^{-4}	-	-
L3	9.38×10^{-4}	-	-
L2:N3 (1:1.2)	5.34×10^{-4}	4.93×10^{-4}	1.08
L3:N3 (1:1.2)	6.29×10^{-4}	3.25×10^{-4}	1.94
L3:N3:PC ₆₁ BM (1:1.2:0.2)	6.73×10^{-4}	6.30×10^{-4}	1.07

10. Surface free energy measurements

The experiments were performed on a Powereach JC2000C2 contact angle goniometer. Droplets of two different liquids, water and ethylene glycol (EG) were cast onto the films with the drop size of 2 μL . Contact angle images were taken at 1 s after the whole droplet was deposited onto the sample surface. The surface free energy of each sample was calculated by:

$$\begin{aligned}\gamma_{\text{water}}(\cos\theta_{\text{water}} + 1) &= 2(\gamma_{\text{sample}}^{\text{d}}\times\gamma_{\text{water}}^{\text{d}})^{1/2} + 2(\gamma_{\text{sample}}^{\text{p}}\times\gamma_{\text{water}}^{\text{p}})^{1/2} \\ \gamma_{\text{EG}}(\cos\theta_{\text{EG}} + 1) &= 2(\gamma_{\text{sample}}^{\text{d}}\times\gamma_{\text{EG}}^{\text{d}})^{1/2} + 2(\gamma_{\text{sample}}^{\text{p}}\times\gamma_{\text{EG}}^{\text{p}})^{1/2} \\ \gamma_{\text{sample}}^{\text{total}} &= \gamma_{\text{sample}}^{\text{d}} + \gamma_{\text{sample}}^{\text{p}}\end{aligned}$$

where θ is the droplet contact angle on the sample film; $\gamma_{\text{sample}}^{\text{total}}$ is the surface free energy of the sample, which is equal to the sum of the dispersion ($\gamma_{\text{sample}}^{\text{d}}$) and polarity ($\gamma_{\text{sample}}^{\text{p}}$) components; $\gamma_{\text{water}} = 72.8 \text{ mJ/m}^2$, $\gamma_{\text{water}}^{\text{d}} = 21.8 \text{ mJ/m}^2$, $\gamma_{\text{water}}^{\text{p}} = 51.0 \text{ mJ/m}^2$, $\gamma_{\text{EG}} = 48.0 \text{ mJ/m}^2$, $\gamma_{\text{EG}}^{\text{d}} = 29.0 \text{ mJ/m}^2$, $\gamma_{\text{EG}}^{\text{p}} = 19.0 \text{ mJ/m}^2$.^[3,4]

Table S11 The contact angles and surface free energy parameters.

Film	Contact Angle ($^{\circ}$)		$\gamma_{\text{sample}}^{\text{d}}$ [mJ/m ²]	$\gamma_{\text{sample}}^{\text{p}}$ [mJ/m ²]	$\gamma_{\text{sample}}^{\text{total}}$ [mJ/m ²]
	Water	Ethylene glycol			
L2	107.84	83.96	19.22	0.45	19.67
L3	108.09	85.98	16.71	0.71	17.42
N3	93.33	82.78	5.77	10.44	16.21

11. NIM certification for L3:N3:PC₆₁BM solar cells

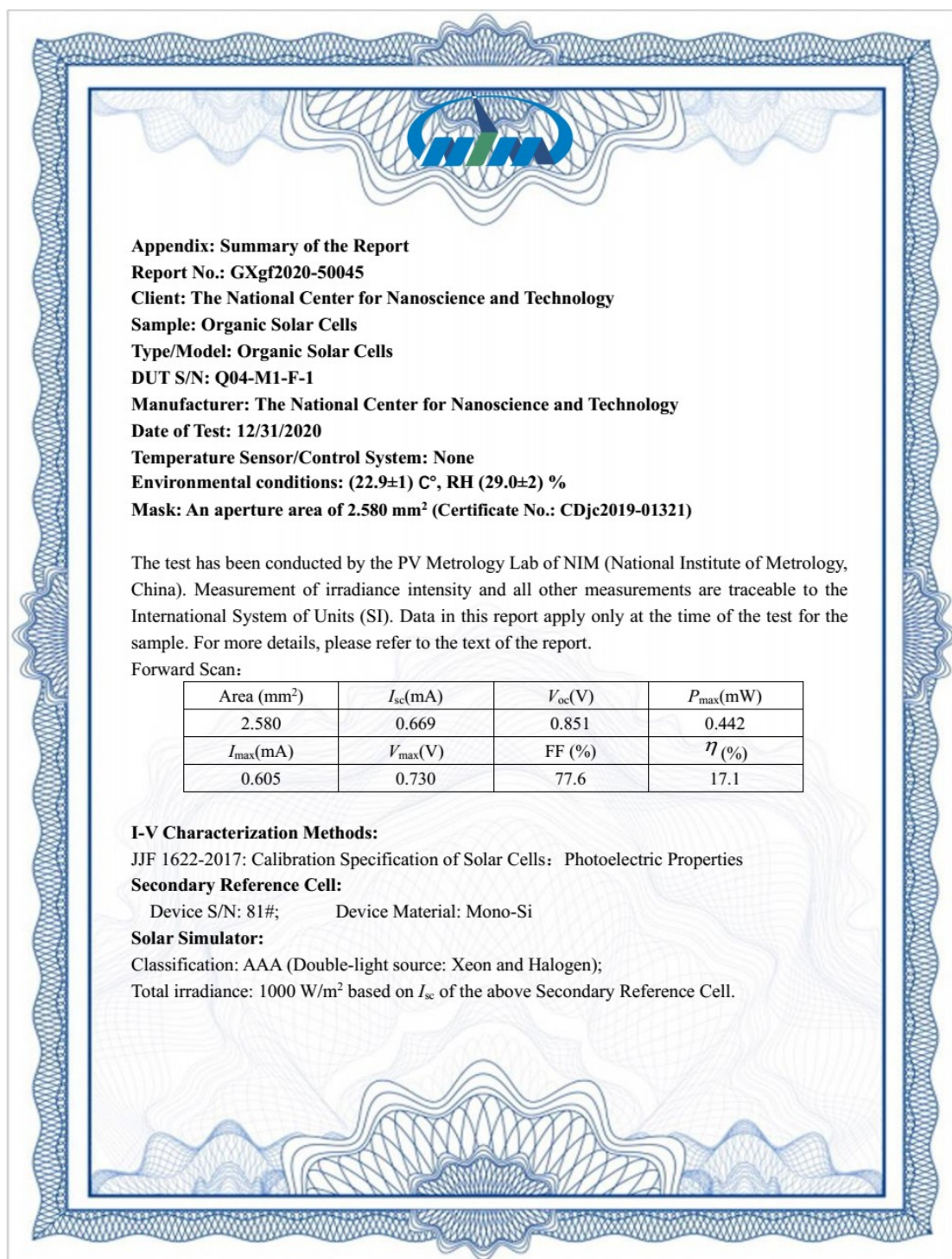


Fig. S17 NIM (Beijing) report for L3:N3:PC₆₁BM solar cells.

12. P_{diss} and P_{coll} for L3:N3:PC₆₁BM solar cells

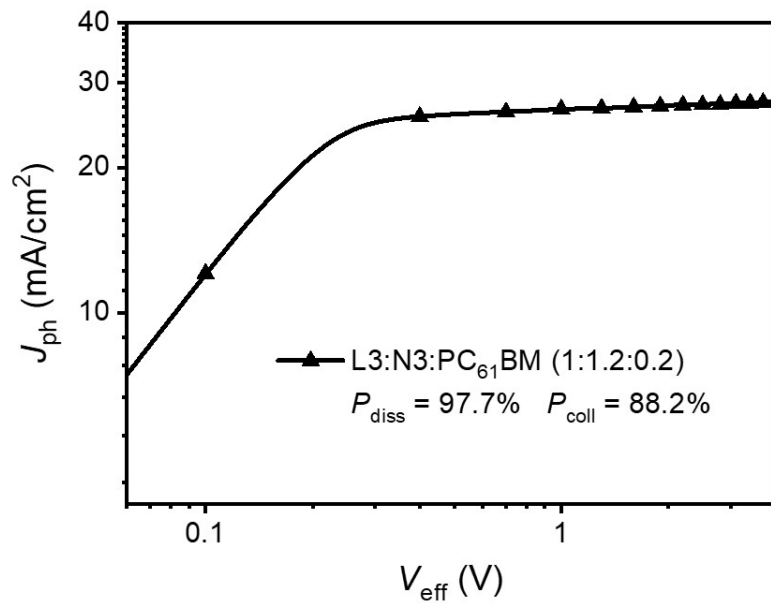


Fig. S18 $J_{\text{ph}}-V_{\text{eff}}$ plot.

13. Bimolecular recombination in L3:N3:PC₆₁BM solar cells

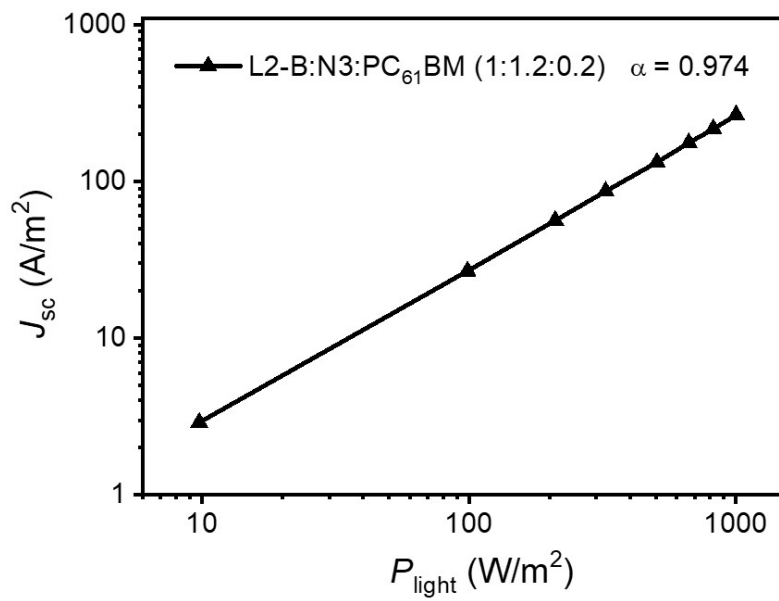


Fig. S19 $J_{\text{sc}}-P_{\text{light}}$ plot.

14. The GIWAXS pattern and AFM images for L3:N3:PC₆₁BM blend film

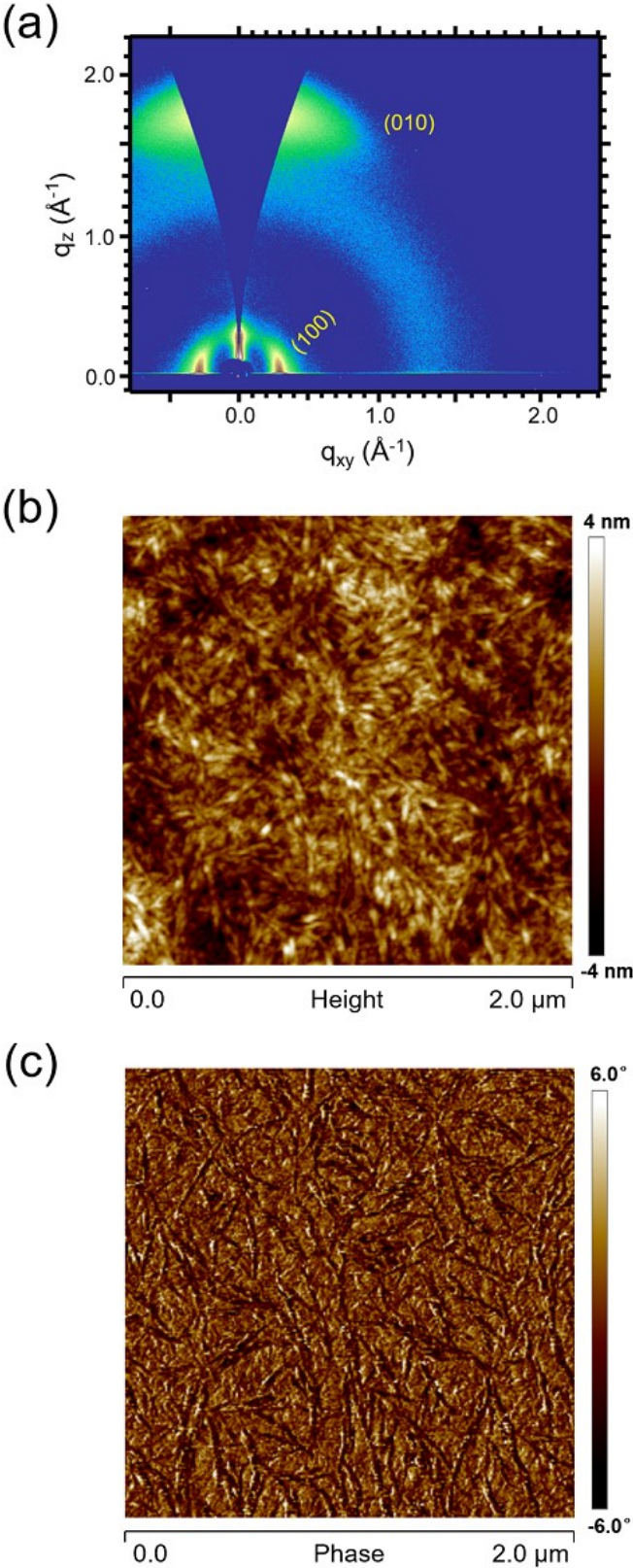


Fig. S20 (a) GIWAXS pattern, (b) AFM height image and (c) AFM phase image for L3:N3:PC₆₁BM (1:1.2:0.2) blend film.

References

- [1] J. Liu, L. Liu, C. Zuo, Z. Xiao, Y. Zou, Z. Jin and L. Ding, *Sci. Bull.*, 2019, **64**, 1655-1657.
- [2] C. Duan, W. Cai, B. B. Y. Hsu, C. Zhong, K. Zhang, C. Liu, Z. Hu, F. Huang, G. C. Bazan, A. J. Heeger and Y. Cao, *Energy Environ. Sci.*, 2013, **6**, 3022-3034.
- [3] D. K. Owens and R. C. Wendt, *J. Appl. Polym. Sci.*, 1969, **13**, 1741-1747.
- [4] M.-C. Michalski, J. Hardy and B. J. V. Saramago, *J. Colloid Interface Sci.*, 1998, **208**, 319-328.